Hybrid-Particulate Composites Based on an Epoxy Matrix, a Reactive Rubber, and Glass Beads: Morphology, Viscoelastic, and Mechanical Properties

A. MAAZOUZ, H. SAUTEREAU, and J. F. GERARD*

Laboratoire des Matériaux Macromoléculaires, URA CNRS No. 507, Institut National des Sciences Appliquées de Lyon, 20, Avenue A. Einstein, 69621 Villeurbanne Cedex, France

SYNOPSIS

The deformation and fracture behaviors of hybrid-particulate epoxy composites have been examined. These materials were based on a DGEBA/DDA matrix with various volume fractions of glass beads and different rubber contents. Young's modulus, yield stress, dynamic mechanical spectra, and fracture energy have been determined at room temperature. The Kerner model fits well the Young's modulus for the hybrid complexes with various glass bead contents. The analysis of the relaxation peak recorded from viscoelastic measurements allow us to discuss the influence of the introduction of the glass beads on the mobility of macromolecular chains and the characteristics of the rubber-separated phase. The fracture energy displays a strong improvement and a synergism effect due to the presence of both kinds of particules. The toughening mechanisms were discussed. © 1993 John Wiley & Sons, Inc.

INTRODUCTION

Thermosets, such as epoxies, are now widely used as structural matrices for high-performance composites according to their stiffness at relatively high temperatures. Another application of such polymers exists on the adhesives in joints. However, according to their highly cross-linked density, the epoxy networks are brittle; thus, they display a rather poor resistance to impact and crack propagation. Numerous works have been carried out on the toughening mechanisms through the introduction of rigid or soft particles.[1,2] The first method is the rubber incorporation, which leads to a phase separation during the curing of the epoxy system.[3,4] In many cases, carboxy-terminated butadiene–acrylonitrile copolymers (CTBN) have been used.[5,6] The resulting morphologies of the dispersed phase can be controlled by the acrylonitrile content of the CTBN rubber and the cure schedule.[7,8] The sizes of the generated particles are usually between 0.2 and 5 μm; the toughening mechanisms could be dependent on the particle size. For very small particles (smaller than 0.1 μm), the shear yielding of the epoxy matrix is the main mechanism, and for larger particles, cavitation at the particle/matrix interface or inside the particle takes place.[4]

The second method consists of the introduction of brittle rigid particles, such as glass beads, silica, or alumina.[2,9–11] Significant improvements of fracture properties are observed by mechanisms such as crack-front pinning. The mechanical behavior of the rigid particulate-filled epoxies are dependent on the properties of each phase (volume fraction, particle size, aspect ratio of the filler, etc.) and also on the matrix–filler adhesion.[2,10,12]

Nevertheless, these two ways for toughening the epoxy resins could sacrifice one property at the expense of another. The introduction of a reactive liquid rubber leads to a decrease in the glass transition temperature of the epoxy matrix, because a part of the rubber remains dissolved in the matrix.[13–15] On the other hand, the introduction of rigid particles induce an increase in the stiffness and the brittleness.

* To whom correspondence should be addressed.

An interesting method concerns the combination of both rigid and rubbery particles.[12,16-20] The same concept can be applied to fibrous composites.[21,22] As reported in different papers,[16-19] the two different toughening mechanisms operating from the two kinds of particles lead to hybrid composite materials. Because the toughness of the hybrid-particulate composites shows the greatest values of G_{Ic}, Kinloch et al.[16-19] deduced that there is a degree of synergism.

Different works have been carried out on the study of hybrid-particulate composites based on hollow glass spheres,[23] zirconia, or alumina fibers.[20,24-28] From the combination of a rigid inorganic filler and a rubber-modified epoxy matrix, materials with desired properties (T_g, modulus) were able to be obtained.

The purpose of the present work is to study the structure–property relationships of hybrid materials based on a rubber-modified DGEBA/dicyandiamide (DDA) network and glass beads. In a previous paper,[13] we showed the influence of the introduction of reactive CTBN rubbers on the morphology, viscoelastic, and mechanical properties of the same epoxy system without filler. On the other hand, the mechanical properties of particulate composites based on an unmodified DGEBA/DDA matrix were described in another paper.[29] The present article describes the influence of both a dispersed rubber phase and glass beads on the thermal, viscoelastic,

and mechanical properties. The effects of the volume fraction of each phase on the morphology and properties are investigated to show if a synergism exists in the case of the combination of two kinds of dispersed phases.
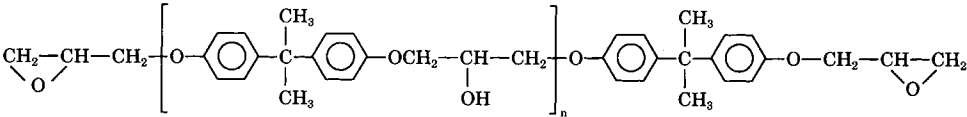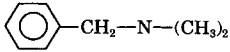
EXPERIMENTAL

Products

The chemical formula of the epoxy prepolymer diglycidyl ether of bisphenol A (DGEBA), the hardener dicyandiamide (DDA), the catalyst benzyl dimethyl amine (BDMA), and the CTBN rubber (R8) are described in Table I. The DDA was previously mixed with DGEBA ($\bar{n} = 0.15$) by the manufacturer (50 : 50 wt).

The structure–property relationships of the BDMA-catalyzed DGEBA/DDA networks (stoichiometric ratio equal to 0.6) were described in a previous paper.[30] The liquid reactive CTBN rubber was introduced as an epoxy-terminated copolymer (ETBN), which was prepared from CTBN and DGEBA.[13,31] The percentage (by weight) of the ETBN elastomer (expressed in terms of CTBN8 content) introduced in the epoxy matrix was varied from 0 to 15%.

A-glass beads from Sovitec with particle sizes ranging from 3 to 70 μm and an average diameter

Table I   Chemical Products Used in the Synthesis of Epoxy Networks

Name	Chemical Formula	Supplier and Tradename
DGEBA	CH_2—CH—CH_2—[O—⟨O⟩—C(CH$_3$)(CH$_3$)—⟨O⟩—OCH_2—CH(OH)—CH_2—]$_n$—O—⟨O⟩—C(CH$_3$)(CH$_3$)—⟨O⟩—O—CH_2—CH—CH_2 $\bar{n} = 0.15; \overline{M_n} = 380$ g Epoxy prepolymer	Bakelite 0164
DDA	H_2N—C=N—C≡N, NH$_2$ Cyanoguanidine or dicyandiamide	Bakelite VE 2560
BDMA	⟨O⟩—CH_2—N—$(CH_3)_2$ Catalyst or initiator	Aldrich
CTBN	HOOC—[(CH_2—CH=CH—CH_2)$_x$—(CH_2—CH)$_y$]$_z$—COOH, CN $\overline{M_n} = 3500$ g; $\overline{F_n} = 1.8$	Hycar CTBN BF Goodrich

of 26 μm (by number) were used without any surface treatment.

Preparation of Composite and Hybrid Materials

As detailed in a previous article,[13] the cure schedule used in this work was 60 min at 120°C followed by 60 min at 180°C. According to the specific nature of the DDA hardener, the precure temperature has a large influence on the final properties of the epoxy network.

Two types of composite materials were fabricated:

- Composites based on the pure epoxy matrix and the glass beads with volume fractions, ϕ_g, from 0 to 30%

- Hybrid materials based on an ETBN-modified epoxy matrix (CTBN content ranging from 0 to 15% by weight) and glass beads (from 0 to 30% vol). These materials were noted $C(x, \phi_g)$, where x represents the initial amount (by wt) of the CTBN rubber, and ϕ_g, the volume fraction of glass. Two series of hybrid materials were studied, $C(15, \phi_g)$ and $C(x, 20)$, in order to separate the influence of each phase.

This article includes the results obtained on unfilled elastomer-modified DGEBA–DDA epoxies and shown in the first part of this study,[13] noted $C(x, 0)$. Plates were made by casting the degassed mixture into a PTFE-coated mold ($180 \times 180 \times 6$ mm^3).

Characterization of the Materials

The characterizations made on these composites and hybrid systems were the same as those made for the unfilled elastomer-modified epoxies described in the first article.[13] The measurements of the glass transition temperatures were performed on a Mettler TA3000 calorimeter under an argon atmosphere (heating rate: 10 K $\cdot$ min^{-1}). The dynamic mechanical properties were studied using a Rheometrics RDA700 apparatus on parallelepipic specimens ($40 \times 1.5 \times 6$ mm^3) and allowed us to obtain the complex shear modulus, G^*, at a frequency of 0.016 Hz as a function of the temperature. The Young's moduli, noted E_{25}, were obtained from a tensile test at room temperature on an Adamel Lhomargy (DY25) testing machine equiped with an EX10 extensometer. The strain rate was 3.3×10^{-4} s^{-1}. The upper yield stress and strain noted σ_y and e_y, respectively, were deducted from compression tests made on the same tensile machine on parallelepiped specimens (20

$\times 10 \times 6$ mm^3) at $\dot{\varepsilon} = 8.3 \times 10^{-3}$ s^{-1}. The yield stress, σ_y, was corrected assuming a constant volume hypothesis according to the following formula:

$$\sigma_{yc} = \sigma_y(1 - e_y)$$

The critical stress intensity factor, K_{Ic}, and the fracture energy, G_{Ic}, were obtained from three-point bending tests performed on single-edge notched specimens (SEN) ($56 \times 12 \times 6$ mm^3) (span-to-length = 48 mm). Cracks of various lengths, a, were machined with a diamond saw and achieved with a razor blade at room temperature.

Using such a procedure, the radius of the crack tip was about 5 μm. K_{Ic} and G_{Ic} were computed from the formulae

$$K_{Ic} = \sigma_c(\pi \cdot a)^{1/2} f\left(\frac{a}{w}\right)$$

$$G_{Ic} = (K_{Ic}^2/E_{25})(1 - \nu^2)$$

where σ_c is the critical stress for the crack propagation, and $f(a/w)$, a form factor,[32] ν is the Poisson's ratio. The fracture mechanisms were analyzed using scanning electron microscopy (SEM) (Jeol 840 A) after a gold sputtering of the surface of broken SEN specimens.

RESULTS AND DISCUSSION

Glass Transition Temperatures and Thermomechanical Properties

To ensure that the curing was completed, all the materials were studied with DSC. Indeed, no residual exothermal effect was detected and the glass temperature remained constant for a first and a second scan, respectively.

The glass transition temperature of the pure epoxy matrix, T_{gE}, is about 144°C, whereas the T_g of the phase-separated rubber, T_{gR}, is about -62°C. These values are listed in Tables II and III.

The introduction of the R8 rubber in the epoxy matrix induces a decrease of the glass transition temperature of the epoxy network. In fact, the T_{gE} of the blend-modified DGEBA–DDA or $C(15,0)$ is only 135°C. This effect is attributed to the plasticization of the epoxy network by a part of the rubber that remains dissolved in the matrix. From the Fox equation, we estimated that 2.7% (vol) of the initial rubber is in the continuous phase.[13] This effect is clearly evidenced on the position of the main relaxation, α_E, of the epoxy matrix (T_{α_E}) (Tables II and

Table II Glass Transition Temperatures, T_{gE}, and Dynamic Mechanical Characteristics of the Composite Materials Based on Unmodified DGEBA/DDA Epoxy Network and Various Volume Fractions of Glass Beads at 0.016 Hz

Material	T_{gE} (°C)	T_{α_E} [a] (°C)	h_{α_E} [b]	σ_{α_E} [c] (°C)	G'_{rub} [d] (MPa)
Matrix	144	153	0.95	8	12.0
C(0, 10)	144	157	0.78	11	11.5
C(0, 20)	146	160	0.64	14	15.3
C(0, 30)	147	162	0.62	14	29.0

[a] At the maximum of the tan δ peak.
[b] Height of the tan δ peak.
[c] Width at half-height of the tan δ peak.
[d] At T_{α_E} + 50°C.

III). On the contrary, the introduction of glass beads in the epoxy (Table II) leads to an increase of the glass transition temperature, T_{gE}. This phenomenon is more important on the temperature of the α_E peak, T_{α_E}, and was previously reported in another article.[29] In fact, the dynamic mechanical characteristics in the glass transition region of the epoxy matrix are very sensitive to the introduction of the glass filler. The increase of T_{α_E} and of the width (at the half-height), σ_{α_E}, could be attributed to the reduction of the mobility of the macromolecular chains in the vicinity of the glass surface, in agreement with the literature.[29,33-35]

Table III Glass Transition Temperatures of the Epoxy Network, T_{gE}, and of the Rubbery Phase, T_{gR}, in the Hybrid Materials and Dynamic Mechanical Characteristics of These Materials at 0.016 Hz in the Glass Transition Region

Material	T_{gE} (T_{gR}) (°C)	T_{α_E} [a] (°C)	h_{α_E} [b]	σ_{α_E} [c] (°C)	G'_{rub} [d] (MPa)
C(15, 0)	135 (−62)	146	0.70	13	7.0
C(15, 10)	136 (−60)	147	0.68	15	8.9
C(15, 20)	141 (−60)	148	0.66	15	11.0
C(15, 30)	139 (−56)	150	0.60	14	23.0
C(0, 20)	146	160	0.64	14	21.0
C(5, 20)	146 ([e])	158	0.69	14	19.5
C(10, 20)	142 (−57)	150	0.64	16	17.7
C(15, 20)	141 (−60)	148	0.66	15	17.0

[a] At the maximum of the tan δ peak.
[b] Height of the tan δ peak.
[c] Width at half-height of the tan δ peak.
[d] At T_{α_E} + 50°C.
[e] Not observed.

The same trend is observed for the hybrid systems based on a rubber-modified epoxy network (15% wt) as the matrix and different amounts of glass beads (Table III). Indeed, slight increases of T_{gE} and T_{α_E} by increasing the volume fraction of glass could be noted. Nevertheless, the effect of the glass beads content is more pronounced on the composites based on an unmodified epoxy network (Fig. 1). The difference between the two series is not important according to the accuracy of the measurements; thus, we can consider that the influence of the volume fraction of glass on the T_{α_E} values is the same. This observation is confirmed by the parallel evolutions of the shear modulus in the rubbery state, G'_r, as a function of ϕ_v (Fig. 2). This parameter was found to be very sensitive to any change in the mobility of the chains in the vicinity of the glass surface.[29] Thus, the effect of the glass beads on the mobility of the unmodified or rubber-modified epoxy matrix is the same. The divergence between the experimental data and a simulation using the Kerner model[36] is observed over 10% vol of glass beads in the two cases, confirming an additional effect that is not taken into account by the modelization. The calculations are made assuming that the matrices remain the same with the addition of glass beads.

In a different way, the same trends are observed on the evolution of the position of the α_E peak, associated with the glass transition temperature of the epoxy, and of the shear modulus in the rubbery state, G'_r, with the initial amount of R8 rubber introduced in the DGEBA–DDA network (Fig. 3). As observed on the blends, T_{α_E} and G'_r decrease by increasing the
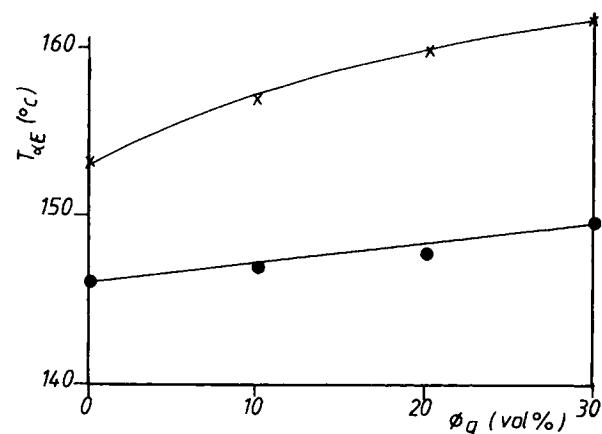

Figure 1 Position of the main relaxation, α_E, of the epoxy network as a function of the volume fraction of glass beads: (✕) unmodified epoxy matrix composites; (●) R8 rubber-modified (15% wt) epoxy matrix hybrids. Frequency: 0.016 Hz.
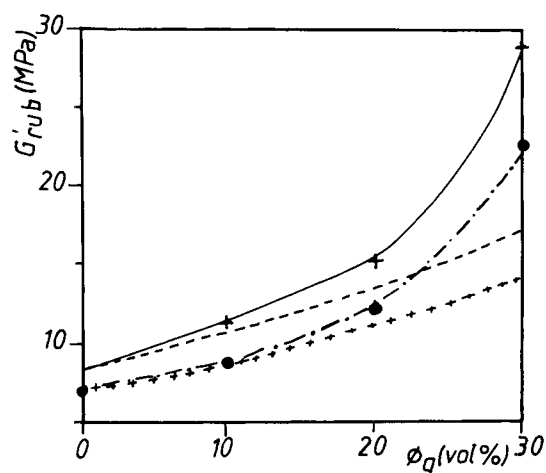
Figure 2 Shear modulus in the rubbery state, G'_r vs. the volume fraction of glass beads in (X) unmodified epoxy matrix composites; (●) R8 rubber-modified (15% wt) epoxy matrix hybrids. Simulation using the Kerner model: (------) composites $C(0,x)$; (+++++) hybrids $C(15, \phi_g)$.
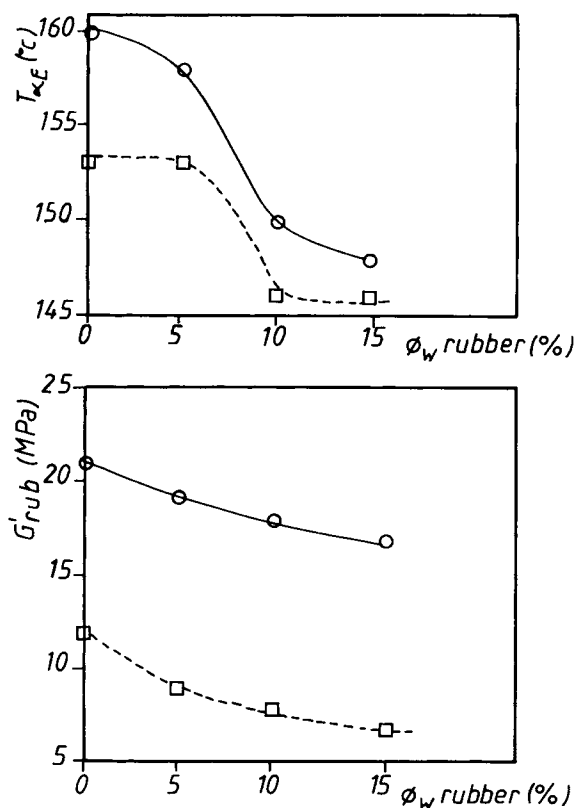
amount of the R8 rubber initially introduced. This effect was attributed to the epoxy continuous phase.[13]

Thus, it could be assumed in all the systems that there is no effect due to the combination of the rubber and the glass beads. This conclusion is confirmed by the study of the morphology of the dispersed phase on the fracture surfaces (Fig. 4). In fact, the average particle diameter is about 1.8 μm for all the materials. In a previous article,[13] a slight increase of the average size, $\bar{D}$, by increasing the rubber content was observed in agreement with the literature.[15,31,37] Nevertheless, the $\bar{D}$ in the case of the R8-modified DGEBA/DDA varied only from 1.5 to 1.9 μm for 5% wt and 15% wt of R8 rubber, respectively. According to (1) the fact that the glass transition temperature, T_{g_E}, is sensitive to the interactions existing between the glass particles and the epoxy chains and (2) the accuracy on the measurement of the volume fraction of the dispersed phase,[13] the

Figure 3 Position of the α_E peak at 0.016 Hz and storage shear modulus in the rubbery state, G'_r, as a function of the initial amount of the R8 rubber introduced in the epoxy matrix; (□) blends from DGEBA/DDA epoxy network and R8 rubber; (○) hybrid systems based on a rubber-modified DGEBA/DDA matrix and 20% vol of glass beads.
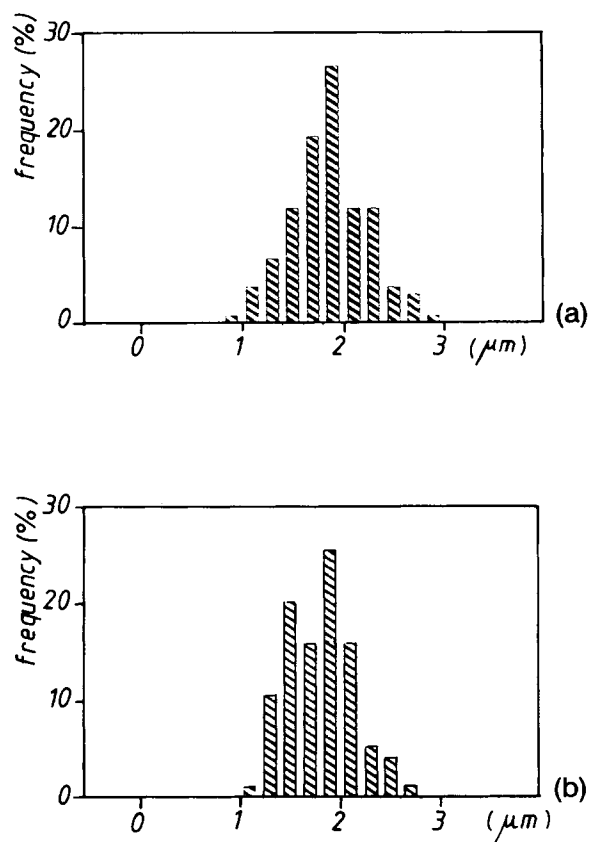

Figure 4 Distributions of the elastomer particles sizes in (a) an elastomer-modified DGEBA–DDA network (15% wt of R8 rubber) and in (b) a hybrid system based on a DGEBA–DDA elastomer-modified (15% wt) matrix and 20% (vol) of glass beads.
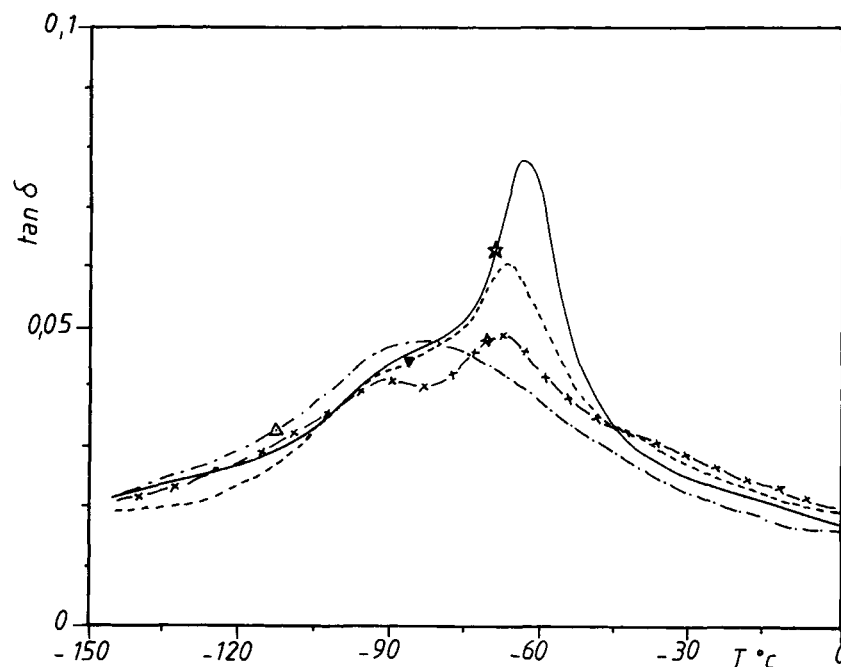
Figure 5 Dynamic mechanical spectra (loss factor, tan δ, vs. temperature) at 0.016 Hz for the hybrid materials based on 20% vol of glass beads and an R8-modified DGEBA–DDA matrix; ($\triangle$) unmodified epoxy matrix; ($\lozenge$) 5% wt of R8 introduced into the epoxy matrix; ($\blacktriangledown$) 10% wt of R8 introduced in the epoxy matrix; ($\star$) 15% wt of R8 introduced into the epoxy matrix.

compositions of each phase (continuous epoxy matrix and elastomer dispersed phase) cannot be calculated. Indeed, it was found that in the R8 rubber-modified DGEBA–DDA systems, the dispersed phase displayed a substructure with a volume fraction of the epoxy copolymer close to 50% in the elastomer particles.[15,38]

In the low-temperature regions (from −150 to 0°C) of the dynamic mechanical spectra, the main relaxation of the phase-separated rubber, α_R, associated with its glass transition and the secondary relaxation, β_E, of the epoxy network are witnessed (Fig. 5). According to the difference in the apparent activation energies of the α_R and β_E relaxations, the measurements are made at a low frequency (0.016 Hz). Even for this frequency, the superposition of the two peaks implies that the characteristics of the α_R relaxation can be determined: temperature, amplitude, h_{α_R}, and the high-temperature component of the width, σ_{α_R} (HT) (Table IV). The position of the α_R peak is more or less the same as for all the hybrid material (about −65°C at 0.016 Hz). The influence of the rubber content and/or the influence of the volume fraction of glass beads should be related to the T_{α_R} values because of the temperature shift of the α_R peak induced by the superposition of

the relaxations. For the same volume fraction of glass beads, the amplitude and σ_{α_R} (HT) increase by increasing the initial amount of rubber, as expected (Table IV). On the other hand, for the same amount of rubber (15% wt) introduced in the epoxy matrix, these parameters, especially h_{α_R}, decrease. Indeed, the volume fraction, ϕ_R^0, of rubber calculated

Table IV   Dynamic Mechanical Characteristics of the Rubber Relaxation in the Hybrid Materials at 0.016 Hz

Material	ϕ_R^0 (%)	T_{α_R}[a] (°C)	h_{α_R}[b] ($\times 10^{-2}$)	σ_{α_R}[c] (°C)
C(15, 0)	17.3	−64	5.6	10
C(15, 10)	15.6	−60	4.7	11
C(15, 20)	13.9	−65	4.3	14
C(15, 30)	12.1	−64	3.3	13
C(0, 20)	—	—	—	—
C(5, 20)	5.0	−67	2.7	—
C(10, 20)	9.3	−67	4.0	13
C(15, 20)	13.9	−65	4.3	14

[a] At the maximum of the tan δ peak.
[b] Height of the tan δ peak.
[c] High-temperature component of the width at half-height of the tan δ peak.

on the total volume decreases weakly by increasing the volume fraction of glass beads (Table IV). For example, in the hybrid system noted C(15,30), (i.e., the material based on an R8-modified (15% wt) epoxy matrix and 30% vol of glass), the rubber represents 12% of the total volume.

Thus, there is no additional effect of the incorporation of the glass and of the reactive rubber on the chemical and physical states of the matrix. For further works, especially on the mechanical behavior, the influence of the volume fraction of glass and/or elastomer could be studied without any consideration on the changes of the chemistry of the matrix (cross-linking, e.g.) or of the characteristics of the elastomer-rich particles.

Elastic and Yielding Properties

The values of the Young's moduli of the various composites and hybrid systems are reported in Tables V and VI. For the composites [noted C(0, ϕ_g)] and for the hybrid composites based on a rubber-modified (15% wt) matrix, as expected, the Young's modulus increases by increasing the volume fraction of glass [Fig. 6(a)].[39] Numerous works have been carried out to explain the dependence of E_{25} upon the volume fraction of rigid particles.[33,40–42] In Figure 6(a), the experimental data are compared to the Kerner model for the composites and the hybrid particulate composites as a function of the volume fraction of glass, ϕ_g. In agreement with a previous study,[39] the model allows us to predict the modulus for the low-volume fraction for composites based on an unmodified matrix. In the case of the hybrids, the model predicts the Young's modulus in all the range of ϕ_g. This observation could be explained by the assumptions of the model. In fact, the Kerner development consists of an average grain surrounded by an average shell of suspending medium; thus, it consists of an average elastic problem.[36] In the case of the hybrid materials, the presence of the rubber particles having a low average diameter could modify the triaxial stress field induced by the glass particles

Table V Mechanical Properties at 25°C (Tension and Compression) for the Composite Systems

Material	E_{25} (GPa)	σ_{yc} (MPa)	e_y (%)
Matrix	2.8	102.6	5.0
C(0, 10)	3.6	107.9	4.5
C(0, 20)	4.8	112.5	5.5
C(0, 30)	6.0	123.0	4.0

Table VI Mechanical Properties at 25°C (Tension and Compression) of the Hybrid Systems

Material	E_{25} (GPa)	σ_{yc} (MPa)	e_y (%)
C(15, 0)	1.76	70.0	4.9
C(15, 10)	2.10	72.0	4.8
C(15, 20)	2.90	75.0	3.9
C(15, 30)	3.20	85.0	4.1
C(0, 20)	4.80	112.0	5.5
C(5, 20)	3.80	101.0	4.8
C(10, 20)	3.60	90.0	4.2
C(15, 20)	2.90	75.0	3.9

and reduce the stress concentrations. The dependence of the Young's modulus upon the glass bead volume fraction could be described using the model developed by Ishai and Cohen.[41] The model consisting of an array of cubic particles surrounded by a shell of matrix gives two bounds. The lower one corresponds to a uniform displacement, and the upper one, to a uniform stress. As can be seen in Figure 6(a), this mechanical model fails to describe the behavior of the composites and the lower bound fits the experimental data for the hybrid-particulate composites. This result is in agreement with the work done by Young et al.[19]

The dependence of E_{25} with ϕ_g is more or less parallel for the blends and for the hybrid composites, showing that the main effect on the stiffness is the glass content. On the contrary, for the same volume fraction of glass beads (20%), the Young's modulus decreases by increasing the amount of the R8 rubber introduced into the epoxy matrix [Fig. 6(b)]. Because of the lack of precision on the true volume fraction of the separated rubber phase, the Kerner model cannot be applied.

The yield behavior of the materials are given in Figure 7(a) and (b) (values are reported in Tables V and VI). A constant shift at lower values of yield stress, σ_{yc}, is observed from the composites based on an unmodified matrix and hybrid materials made from a rubber-modified matrix (15% wt) [Fig. 7(a)]. On the other hand, a constant shift to higher values of σ_{yc} is noted when a constant volume fraction of glass beads (20%) is added to a rubber-modified DGEBA/DDA network [Fig. 7(b)]. Thus, there is a simple additional effect of glass beads and rubber on the yield stress. This behavior is explained by the fact that the yielding is governed mainly by the shear yielding of the epoxy matrix in all the materials. The volume fraction of glass and/or the amount of rubber, in our case, only affects the values of the yield stress.
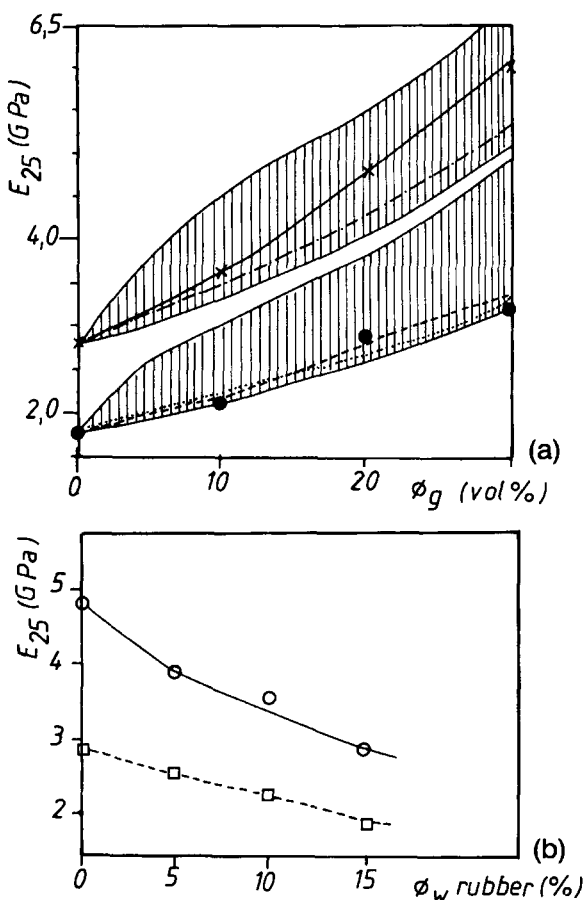
Figure 6 (a) Young's modulus measured at room temperature vs. the volume fraction of glass beads for (X) composites based on unmodified epoxy matrix and (●) hybrid composites based on a 15% R8-modified epoxy matrix. (— · — · — ·) and (. . . . .) are the simulations using the Kerner model for the composites and the hybrid systems, respectively (the hatched zone represents the gap between the lower and upper bounds of the Ishai and Cohen model). (b) Young's modulus measured at room temperature for (□) the rubber-modified epoxies and (○) the hybrid composites based on 20% vol of glass beads.

Fracture Properties

For all the materials studied in this article, the crack propagation is stable-brittle, corresponding to the type C described by Bascom and Hunston.[32] Thus, in this testing mode, i.e., single-edge notched specimens at 25°C and for the strain rate used, no evidence of stick-slip is noted. The behavior of the hybrid-particulate composites is the same as for composites,[39] blends,[13] or pure matrices[30] based on a DGEBA–DDA system. Kinloch et al.[17] found some changes from an unstable-brittle (Type B) crack propagation at low temperature to a stable-ductile

crack growth at high temperatures for hybrid-particulate composites tested in the double-torsion mode. The crack-propagation behavior is ascribed in this case to the crack-tip blunting.[43] The failure mechanisms are discussed later and compared to those reported in the literature.

The values of the critical stress intensity factor, K_{Ic}, and of the fracture energy, G_{Ic}, are shown in Tables VII and VIII. The critical stress intensity factor, K_{Ic}, increases linearly by increasing the volume fraction of glass beads [Fig. 8(a)]. Such a dependence was observed in numerous works.[10,12,20,39] The dependence of G_{Ic} with ϕ_g is quite similar for the composites [Fig. 9(a)]. In a previous study[38] and in agreement with other papers,[11,44] a maximum was found for G_{Ic} at 20% vol of glass. The different values and dependence are attributed to the method for making the notch. In this case, the crack-tip is more accurate.
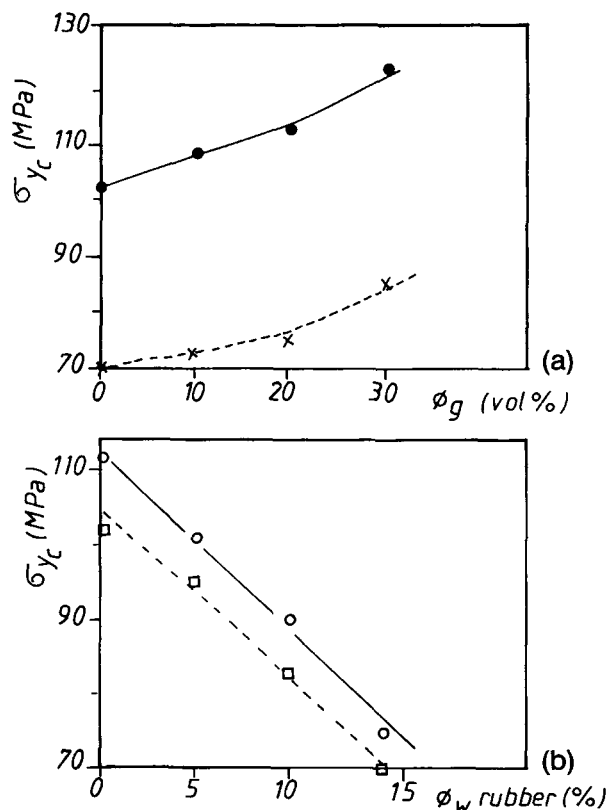

Figure 7 (a) Yield stress, σ_{yc}, as a function of the volume fraction of glass beads for (●) the composites based on an unmodified epoxy matrix and (X) the hybrid systems based on a 15% R8-modified epoxy matrix. (b) Yield stress, σ_{yc}, as a function of the initial amount of R8 rubber for (□) the rubber-modified epoxies and (○) the hybrid systems based on 20% vol of glass beads.

Table VII   Fracture Properties at 25°C of Composite Materials Based on an Unmodified Epoxy Matrix and Different Volume Fractions of Glass Beads

Material	K_{Ic} (MPa m$^{1/2}$)	G_{Ic} (J m^{-2})	r_p (μm) Dugdale	r_p (μm) Irwin
Matrix	0.70	130	18.5	2.4
C(0, 10)	1.00	240	33.7	4.5
C(0, 20)	1.46	390	69.8	9.4
C(0, 30)	2.00	620	103.7	14

Table VIII   Fracture Properties at 25°C of Hybrid-Particulate Composite Materials

Material	K_{Ic} (MPa m$^{1/2}$)	G_{Ic} (J m^{-2})	r_p (μm) Dugdale	r_p (μm) Irwin
C(15, 0)	1.33	870	142	18
C(15, 10)	1.72	1240	222	30
C(15, 20)	2.48	1920	429	58
C(15, 30)	2.53	1600	348	47
C(0, 20)	1.46	390	67	9
C(5, 20)	1.46	510	82	17
C(10, 20)	2.53	1570	310	35
C(15, 20)	2.48	1920	429	58

The behavior of the hybrid-particulate composites based on a rubber-modified epoxy matrix is quite different [Figs. 8(a) and 9(a)] with the increase of the volume fraction of glass. At over 20% vol for ϕ_g, K_{Ic} seems to be constant and the fracture energy,

G_{Ic}, displays a maximum. These results are in agreement with those reported in different articles.[12,17]

For the particulate-filled epoxy materials, the toughening mechanisms reported in the literature are crack-pinning and crack-blunting. On an un-
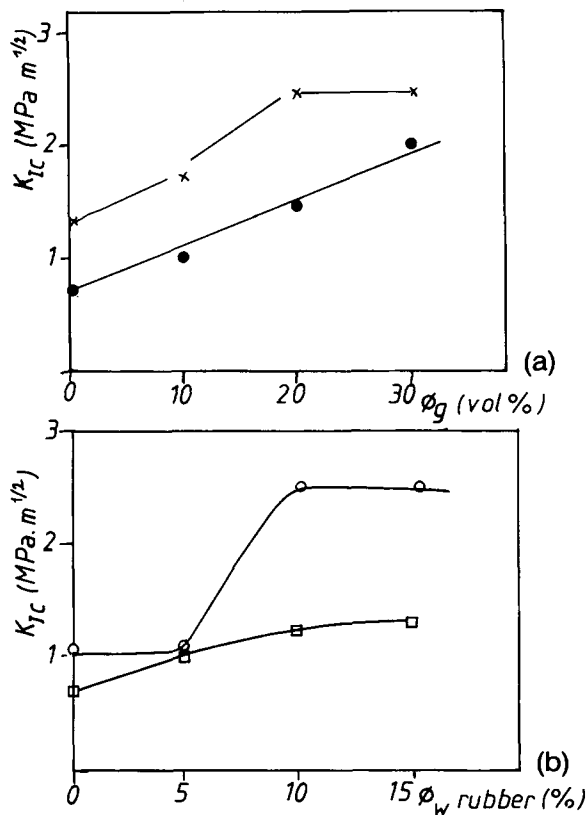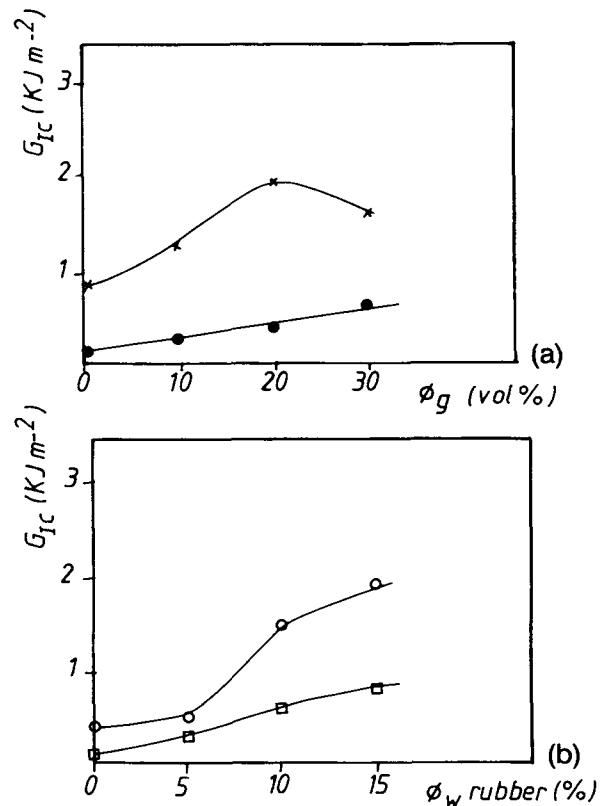

Figure 8   (a) K_{Ic} at 25°C vs. the volume fraction of glass beads for (●) the composite materials based on an unmodified matrix and (X) the hybrid-particulate composites based on a rubber-modified epoxy matrix (15% wt). (b) K_{Ic} at 25°C vs. the initial amount of R8 rubber in (□) blends and (○) hybrid composites based on 20% vol of glass beads.

Figure 9   (a) Fracture energy, G_{Ic}, vs. the volume fraction of glass beads for (●) composites and (X) hybrid-particulate composites based on a rubber-modified matrix (15% wt). (b) Fracture energy, G_{Ic}, vs. the initial amount of R8 rubber for (□) blends and (○) hybrid composites based on 20% vol of glass beads.
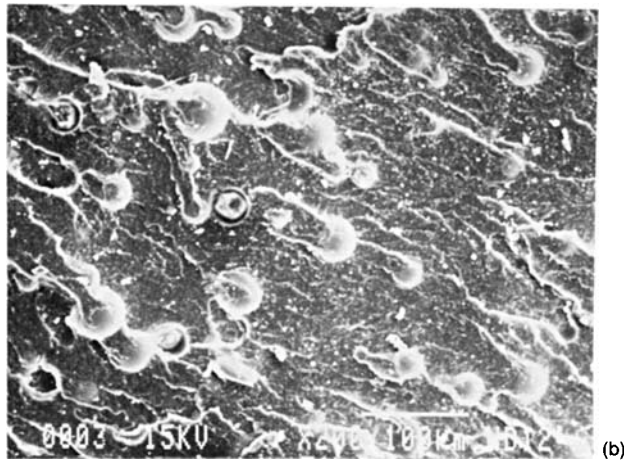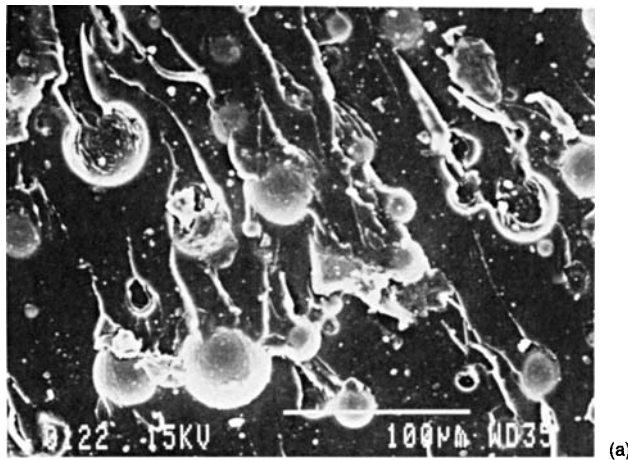
Figure 10 Scanning electron microscopy: (a) fracture surfaces of a composite based on an unmodified matrix and 20% vol of glass beads; (b) hybrid-particulate composite based on 20% vol glass beads and a rubber-modified (15% wt) matrix.

modified epoxy matrix filled with glass beads, the existence of the crack-pinning mechanism was the main toughening effect.[10,12] The evidence of such a mechanism is shown by the presence of tails behind the particles on the fracture surfaces [Fig. 10(a)]. For the hybrid-particulate composites, crack-pinning is not sufficient to explain the high values of the critical stress intensity factor or of the fracture energy. In this case, crack-tip blunting is involved. In fact, according to Kinloch and Williams,[45] crack-

blunting is favored when the yield stress, σ_y, is lower than 100 MPa, which is the case of all of the hybrid systems [Fig. 7(a) and 7(b)]. The fracture surfaces of hybrid-particulate materials [Fig. 10(b)] display many secondary microcracks that result from the shear yielding of the matrix. Thus, it could be considered in such materials that the two mechanisms coexist: the crack-pinning involved mainly from the presence of the glass beads and the crack-blunting from the elastomer dispersed phase. The cavitation of the rubber particles could be added as a possible toughening contribution, but this was not seen here.

Some theoretical models have been developed to describe the crack propagation through a material filled with particles.[46,47] Lange and Radford[9] proposed a relation between the fracture energy and the average interparticle distance ($\overline{D_S}$):

$$G_{\text{Ic}} = G_{\text{Ic}(0)} + 2W_L/\overline{D_S}$$

where W_L is the line energy per unity length, and $G_{\text{Ic}(o)}$, the fracture energy of the unfilled matrix. $\overline{D_S}$ is expressed as $2\bar{d}\,(1 - \phi_g)/3\phi_g$, where $\bar{d}$ is the mean diameter of the glass beads.[47]

The model fits the experimental data for the composites (with an unmodified matrix) but not for the hybrid materials (Fig. 11). Thus, for these materials, additional toughening mechanisms need to be considered. As explained previously, the presence of rubber particles greatly enhances the extent of the localized plastic-shear deformation at the crack-tip. This one could be quantified using the Dugdale
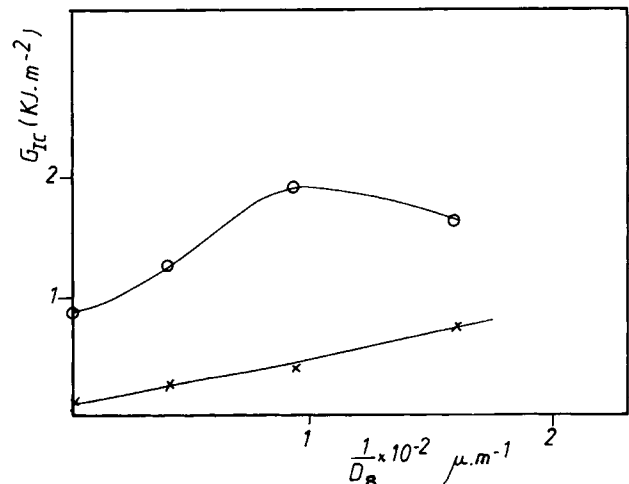

Figure 11 Fracture energy, G_{Ic}, as a function of the reciprocal of interparticle distance, $\overline{D_S}^{-1}$, for (X) the composites and (O) hybrid materials based on a rubber-modified matrix (15% wt).

or Irwin models[48] to compute the radius of the plastic zone, r_p (Tables VII and VIII). A significant increase of r_p is observed when the elastomer is introduced as a dispersed phase in the epoxy matrix. Thus, the crack-tip blunting is involved and reduces the stress concentration at the crack tip. The crack-tip blunting could be quantified[2] through the value of the crack-opening displacement, δ_{tc}[32]:

$$\delta_{tc} = K_{Ic}^2 / E_{25} \cdot \sigma_{yt}$$

where σ_{yt} is the upper yield stress in tension and could be expressed as[49]

$$\sigma_{yt} = 0.75 \cdot \sigma_{yc}$$

δ_{tc} is found to be equal to 5 μm for the composites and 25 μm for the hybrid-particulate materials based on a rubber-modified epoxy matrix (Fig. 12). The results show the importance of localized plastic deformation in increasing the toughness and are in agreement with other studies.[18]

Recently, Pearson and Yee[4] proposed that the particle-size efficiency could be compared to the plastic-zone radius. Thus, particle size larger than r_p acts as bridging particles. Particles smaller than r_p could cavitate and promote shear yielding. On the other hand, the fracture properties of hybrid-particulate composites based on the same volume fraction of glass (20% vol) increase by increasing the amount of R8 rubber in the epoxy matrix [Figs. 8(b) and 9(b)].
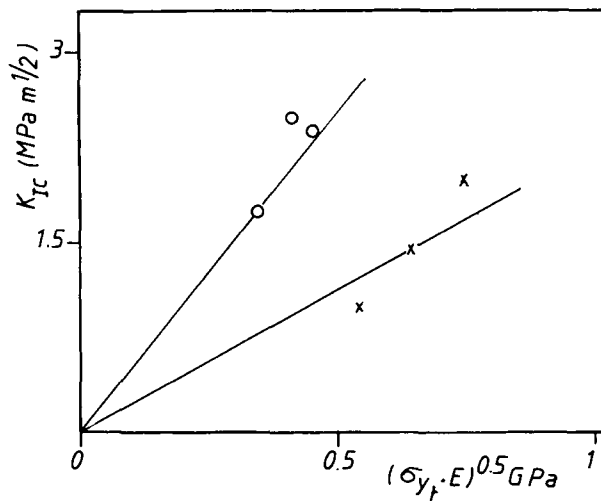
Figure 13 Stiffness, E_{25} (Young's modulus) vs. toughness, K_{Ic} (critical stress intensity factor) for all the composites and hybrid materials at 25°C: (X) unmodified epoxy matrix composites; (●) R8 rubber-modified (15% wt) epoxy matrix hybrids; (□) blends of R8 rubber and epoxy matrix; (O) hybrid systems based on a rubber-modified DGEBA/DDA matrix and 20% vol of glass beads.

On the K_{Ic} plot vs. the amount of rubber, a change of K_{Ic} is noted between 5 and 10% wt of rubber. This effect could be attributed to the coexistence of different toughening mechanisms over 10% of rubber. As demonstrated previously, the toughening effects of rubber particles, especially from the crack-tip blunting, become important. An additive explanation may be proposed, following Pearson and Yee.[4] Glass beads (26 μm) induce a stress field overlap on a larger scale and thus promote cavitation of small rubber particles in the vicinity, which is one of the main sources of shear yielding. As a result, the influence on the fracture properties is not simply an addition.

Thus, by changing the amount of reactive rubber in the epoxy matrix or/and the volume fraction of glass beads, hybrid-particulate composites with desired properties could be obtained (Fig. 13). As a matter of fact, in many applications such as adhesives or matrices for composites, a compromise between stiffness and toughness is necessary. Work is now in progress to test these formulations as adhesives.

Figure 12 Variation of K_{Ic} with $(E \cdot \sigma_{yt})^{1/2}$ for (X) the composites and (O) the hybrid composites based on a rubber-modified matrix (15% wt).
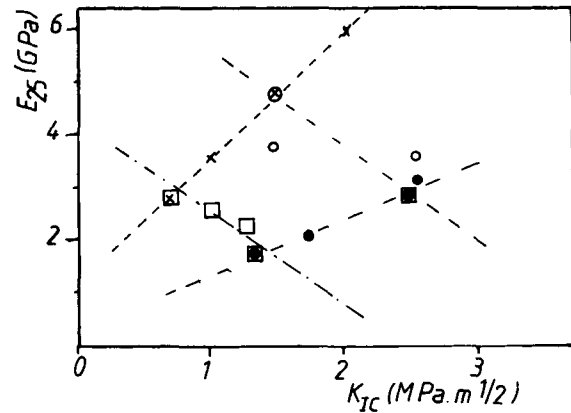
REFERENCES

1. A. J. Kinloch, in *Structural Adhesives*, A. J. Kinloch, Ed., Elsevier, London, 1986, p. 127.
2. R. J. Young, in *Structural Adhesives*, A. J. Kinloch, Ed., Elsevier, London, 1986, p. 163.
3. R. Drake and A. R. Siebert, *Sampe Q.*, **6**, 11 (1975).

4. R. A. Pearson and A. F. Yee, *J. Mater. Sci.,* **26,** 3828 (1991).

5. C. K. Riew, E. H. Rowe, and A. R. Siebert, in *Toughness and Brittleness of Plastics,* R. D. Deanin and A. M. Crugnola, Eds., Advances in Chemistry, Series 154, American Chemical Society, Washington, DC, 1976, p. 326.

6. F. J. McGarry and A. M. Willner, *Org. Coat. Plast. Chem.,* **28,** 512 (1968).

7. L. T. Manzione, J. K. Gillham, and C. A. McPherson, *J. Appl. Polym. Sci.,* **26,** 889 (1981).

8. L. T. Manzione, J. K. Gillham, and C. A. McPherson, *J. Appl. Polym. Sci.,* **26,** 907 (1981).

9. F. F. Lange and K. C. Radford, *J. Mater. Sci.,* **6,** 1197 (1971).

10. A. C. Moloney, H. H. Kausch, and H. R. Steiger, *J. Mater. Sci.,* **18,** 208 (1983).

11. L. J. Broutman and S. Sahu, *Mater. Sci. Eng.,* **8,** 98 (1971).

12. A. C. Moloney, H. H. Kausch, T. Kaiser, and H. R. Beer, *J. Mater. Sci.,* **22,** 381 (1987).

13. A. Maazouz, H. Sautereau, and J. F. Gérard, *Polym. Networks Blends,* **2**(2), 65 (1992).

14. W. H. Lee, K. A. Hood, and W. W. Wright, in *Rubber Toughened Plastics,* Advances in Chemistry Series 222(11), C. K. Riew, Ed., American Chemical Society, New Orleans, 1989, p. 263.

15. D. Verchère, J. P. Pascault, H. Sautereau, S. M. Moschiar, C. C. Riccardi, and R. J. J. Williams, *J. Appl. Polym. Sci.,* **42,** 701 (1991).

16. D. L. Maxwell, R. J. Young, and A. J. Kinloch, *J. Mater. Sci. Lett.,* **3,** 9 (1984).

17. A. J. Kinloch, D. L. Maxwell, and R. J. Young, *J. Mater. Sci.,* **20,** 4169 (1985).

18. A. J. Kinloch, D. L. Maxwell, and R. J. Young, *J. Mater. Sci. Lett.,* **4,** 1276 (1985).

19. R. J. Young, D. L. Maxwell, and A. J. Kinloch, *J. Mater. Sci.,* **21,** 380 (1986).

20. A. C. Roulin-Moloney, W. J. Cantwell, and H. H. Kausch, *Polym. Compos.,* **8**(5), 314 (1987).

21. L. Penn, B. Morra, and E. Mones, *Composites,* **8,** 23 (1977).

22. H. Zhang, L. A. Berglund, and M. Ericson, *Polym. Eng. Sci.,* **31**(14), 1057 (1991).

23. D. A. Tod and S. V. Wolfe, in *Deformation, Yield and Fracture of Polymers VII,* Plastic and Rubber Institute, Cambridge, UK, Apr. 11–14, 1988, p. 98/1.

24. A. C. Garg and Y. W. Mai, *Compos. Sci. Technol.,* **31,** 179 (1988).

25. A. C. Garg and Y. W. Mai, *Compos. Sci. Technol.,* **31,** 225 (1988).

26. I. M. Low, Y. W. Mai, S. Bandyopadhayay, and V. M. Silva, *Mater. Forum,* **10**(4), 241 (1987).

27. I. M. Low and Y. W. Mai, *Compos. Sci. Technol.,* **33,** 191 (1988).

28. S. Bandyopadhyay, *Mater. Sci. Eng.,* **A125,** 157 (1990).

29. N. Amdouni, H. Sautereau, and J. F. Gérard, *J. Appl. Polym. Sci.,* **45,** 1799 (1992).

30. N. Amdouni, H. Sautereau, J. F. Gérard, and J. P. Pascault, *Polymer,* **31,** 1245 (1990).

31. P. Bartlet, J. P. Pascault, and H. Sautereau, *J. Appl. Polym. Sci.,* **30,** 2955 (1985).

32. W. D. Bascom and D. L. Hunstson, *Mater. Sci. Eng.,* **2,** 135 (1971).

33. J. Chauchard, B. Chabert, P. Jeanne, and G. Nemoz, *J. Chim. Phys.,* **84**(2), 239 (1987).

34. P. S. Chua, in *42nd Annual Conference on Composite Materials,* Inst. SPI, Feb. 2–6, 1987, Vol. 21A, p. 1.

35. T. B. Lewis and L. E. Nielsen, *J. Appl. Polym. Sci.,* **14**(6), 1449 (1970).

36. E. H. Kerner, *Proc. Phys. Soc.,* **69B,** 808 (1956).

37. L. C. Chan, J. K. Gillham, A. J. Kinloch, and S. J. Shaw, in *Rubber Modified Thermoset Resins,* Advances in Chemistry Series 208, C. K. Riew and J. K. Gillham, Eds., American Chemical Society, Washington, DC, 1986, p. 193.

38. W. A. Romanchik, J. E. Sohn, and J. F. Geibel, in *Epoxy Resin Chemistry II,* ACS Symposium Series 221, R. S. Bauer Ed., American Chemical Society, Washington, DC, 1983, p. 85.

39. N. Amdouni, H. Sautereau, and J. F. Gérard, *J. Appl. Polym. Sci.,* **46,** 1723 (1992).

40. J. D. Halpin and J. L. Kardos, *Polym. Eng. Sci.,* **16,** 344 (1979).

41. O. Ishai and L. J. Cohen, *Int. J. Mech. Sci.,* **9,** 539 (1967).

42. Z. Hashin and S. Shtrickman, *J. Mech. Phys. Solids,* **11,** 127 (1963).

43. A. J. Kinloch and R. J. Young, in *Fracture Behaviour of Polymers,* Applied Science, London, 1983, p. 421.

44. J. Spanoudakis and R. J. Young, *J. Mater. Sci.,* **19,** 473 (1984).

45. A. J. Kinloch and J. G. Williams, *J. Mater. Sci.,* **15,** 987 (1980).

46. A. G. Evans, *Philos. Mag.,* **26,** 1327 (1972).

47. D. J. Green, P. S. Nicholson, and J. D. Embury, *J. Mater. Sci.,* **14,** 1657 (1979).

48. J. G. Williams, in *Fracture Mechanics of Polymers,* Ellis Horwood, Chichester, 1984.

49. A. S. Wronski and M. Pick, *J. Mater. Sci.,* **12,** 28 (1977).